PPr801 Project Report
on

Rotation-induced nucleon pair breaking in nuclei with quadrupole and octupole deformations

submitted by

Sangram Keshari Patro
Roll no: P0191340

Under the Guidance of

Dr. Sujit Tandel

Department of Physical Sciences
Centre for Excellence in Basic Sciences
(UM-DAE-CBS) Mumbai-400 098

April 2023

Certificate

This is to certify that CEBS student **Sangram Keshari Patro** has undertaken project work from 01/01/23 to 30/04/23 under the guidance of **Dr. Sujit Tandel** and affiliation: **UM-DAE Centre for Excellence in Basic Sciences**. This submitted project report titled **Rotation-induced nucleon pair breaking in nuclei with quadrupole and octupole deformations** is towards the academic requirements of the M.Sc. program's 8th Semester Project Course at UM-DAE CEBS.

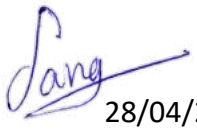

28/04/23

Sangram Keshari Patro

Name & Signature of Student with Date

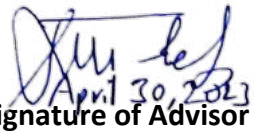

Name & Signature of Advisor (s) with Date

Acknowledgment

I take this opportunity to express my sincere gratitude to Prof. Sujit Tandel who has guided me patiently through this project which has been an extremely fruitful learning experience. I want to thank him for introducing me this wonderful topic of study that has not only kindled interest in me but has also changed the perspective towards several other interests. I also want to thank Saket Suman for his constant support through out the project.

Abstract

The study of nuclear structure attempts to elucidate the unifying mechanisms by which these rich patterns of behaviour emerge from the common underlying strong nuclear interaction between the nucleons (protons and neutrons) that form the nucleus. We have discussed various models to understand the nucleus. Out of the many models, we focus on the Deformed-Shell Model,Fermi gas model and Liquid-drop model. Different model approaches try to accentuate various aspects of nuclear structure in a simple and schematic way. No single model, as yet, is detailed enough to encompass all aspects of the nucleus.

We seek different types of potentials to explain the shell structure and the magic numbers. Then we discuss how we moved from Spherical-Shell Model to Deformed-Shell Model. We also discuss collective nuclear rotation and Cranking model. We have performed extensive theoretical calculations of the rotational frequencies associated with nucleon pair breaking owing to the fast rotation of nuclei with both quadrupole and octupole deformations. The cranking model with the universal parameterization of the Woods-Saxon potential has been used. These calculations explore a region in the nuclear chart of contemporary interest.

Contents

1 Introduction

A tremendous amount of progress in the study of atomic energy levels has been possible because the mathematical form of coulomb's law is known. Whereas, the mathematical form of the nuclear force is not yet known and a simple form (such as a potential function dependent only on the separation of two nucleons) is not a possible solution to the problem. In the absence of detailed information about the nuclear force, theoretical descriptions of nuclei have been centered on models for nuclear structure which are admittedly inadequate but which represent to some extent the observed phenomena. Among the models currently in use in nuclear physics are the Fermi-gas model, the liquid-drop model, the collective model, the shell model, the cluster model, the optical model, the direct reaction model, and the standard model of elementary particles and fundamental interactions. Nuclear models can be divided into two categories.

1. Models with strong interaction between the nucleons:

- Liquid drop model
- α-cluster model
- Shell model

2. Models of non-interacting nucleons:

- Fermi gas model
- Optical model

Some models are discussed below.

2 The liquid drop model

This model treats the nucleus as a drop of incompressible nuclear fluid. It was first proposed by George Gamow and developed by Niels Bohr and John Archibald Wheeler. The fluid is made of nucleons (protons and neutrons), which are held together by the strong nuclear force. This is a crude model that does not explain all the properties of the nucleus, but

- does explain the spherical shape of most nuclei.
- It also helps to predict the binding energy of the nucleus.

The parameterisation of nuclear masses as a function of A and Z, which is known as the **semi-empirical mass formula,** was was first introduced in 1935 by German physicist Carl Friedrich von Weizsäcker: $M(A,Z) = Zm_p + Nm_n - E_B$. where, E_B is the binding energy of the nucleus and is given by:

$$E_B = \underbrace{a_V \cdot A}_{\text{Volum term}} - \underbrace{a_S \cdot A^{\frac{2}{3}}}_{\text{Surface term}} - \underbrace{a_C \cdot \frac{Z^2}{A^{\frac{1}{3}}}}_{\text{Coulomb term}} - \underbrace{a_{Sym} \cdot \frac{(N-Z)^2}{A}}_{\text{Assymetry term}} - \underbrace{\frac{\delta}{A^{1/2}}}_{\text{Pairing term}}$$

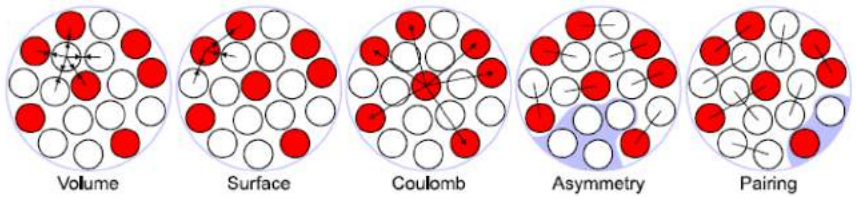

Figure 1: Binding energy of the nucleus. Where the empirical parameters are: $a_V \approx 16$ MeV, $a_S \approx 20$ MeV, $a_C \approx 0.72$ MeV, $a_{Sym} \approx 21$ MeV. And

$$\delta = \begin{cases} -11.2 \text{ Mev}/c^2 & \text{for even Z and N (even-even nuclei)} \\ 0 \text{ Mev}/c^2 & \text{for even Z and N (odd-even nuclei)} \\ +11.2 \text{ Mev}/c^2 & \text{for even Z and N (odd-odd nuclei)} \end{cases}$$

- **Volume term**

The basis for this term is the strong nuclear force. Because the number of pairs that can be taken from A particles is ${}^{A}C_2 = A(A-1)/2$, one might expect a term proportional to A^2 . However, the strong force has a very limited range, and a given nucleon may only interact strongly with its nearest neighbors and next nearest neighbors. Therefore, the number of pairs of particles that actually interact is roughly proportional to A. This term is analogous to the latent heat of evaporation is proportional to the drop mass and as it is defined as the average energy required to disperse the liquid drop into a gas.

- **Surface term**

A nucleon at the surface of a nucleus interacts with less number of nucleons than one in the interior of the nucleus, so its binding energy is less. This can also be thought of as a surface tension term, and indeed a similar mechanism creates surface tension in liquids. So, more the surface area more unstable the system becomes i.e. energy lost due to binding is less. Hence, the surface energy term is therefore negative and is proportional to the surface area ($S = \pi R^2 \sim A^{\frac{2}{3}}$).

- **Coulomb term**

The basis for this term is the electrostatic repulsion between protons. The electric repulsion between each pair of protons in a nucleus contributes toward decreasing its binding energy, hence the -ve sign. From QED we know interaction energy for the charges q_1, q_2 inside the ball is $E_{int} \sim \frac{q_1 . q_2}{R}$. So, $E_C \sim \frac{Z^2}{A^{\frac{1}{3}}}$.

- **Assymmetry term**

It is the increase in energy required by nucleus to have unequal numbers of protons (Z) and neutrons (N). The binding energy of these nuclei will be maxima when nucleons occupy the lowest possible orbital i.e. for symmetric distribution $Z = N = A/2$. But for another repartition,

$$\boldsymbol{N = A/2 + \upsilon, Z = A/2 - \upsilon} \implies \upsilon = \frac{N-Z}{2} = \frac{A-2Z}{2}$$

which involve lifting particles from occupied into empty orbital above that energy level i.e. the system energy increases resulting in decrease in binding energy which explains the -ve sign in the asymmetry term. If the average energy separation between adjacent orbital is taken to be Δ, replacing υ nucleons will cost an energy loss of $\Delta BE = \upsilon(\Delta\upsilon/2)$ (See the figure). The spacing between the highest empty energy level and highest occupied energy level is $\frac{\upsilon}{2} \times$ spacing between adjacent orbital(i.e. Δ) and No. of nucleons are υ So, net change in BE $= \frac{\upsilon}{2} \times \Delta \times \upsilon = \frac{\upsilon^2}{2}\Delta = \frac{(A-2Z)^2}{8}\Delta$. The potential depth describing the nuclear well does not vary much with changing mean number So, energy spacing Δ should vary inversely to fit in more levels in that same potential well. i.e. $\Delta \propto \frac{1}{A}$. So, Assymmetry term becomes $\sim \frac{(A-2Z)^2}{A}$.

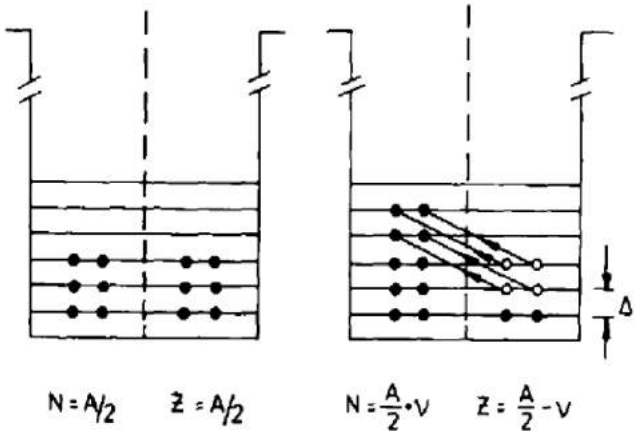

Figure 2: Schematic single-particle model description, two different distributions of A nucleons over the proton and neutron orbital with two-fold (spin) degeneracy. For the drawn figure $\upsilon = 4$ So, the $\Delta BE = \frac{4}{2} \times \Delta \times 4 = 8\Delta$.

- **Pairing term**

  An energy which is a correction term that arises from the effect of **spin-coupling**. Due to the Pauli exclusion principle the nucleus would have a lower energy if the number of protons with spin up will be equal to the number of protons with spin down. This is also true for neutrons. Only if both Z and N are even, both protons and neutrons can have equal numbers of spin up and spin down particles. Hence even no. of particles is more stable ($\delta < 0$ for even-even nuclei) than an odd number ($\delta > 0$).

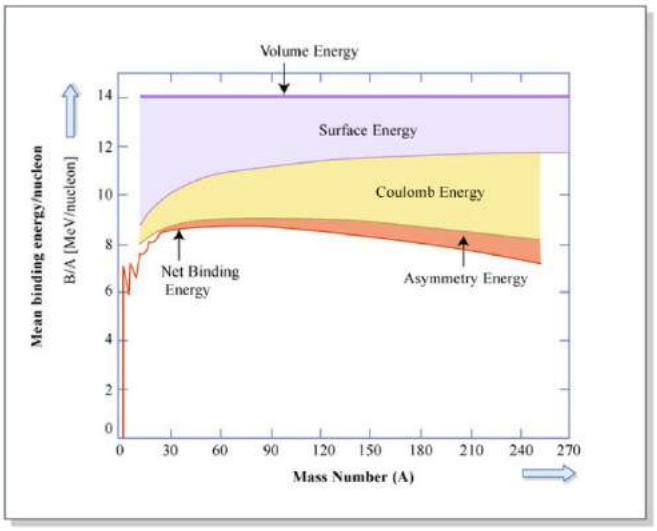

Figure 3: The different contributions to the binding energy per nucleon versus mass number A. The contributions of the asymmetry and Coulomb terms increase rapidly with A, while the contribution of the surface term decreases.

3 Fermi-Gas Model

The theoretical concept of a Fermi-gas may be applied for systems of weakly interacting fermions, i.e. particles obeying Fermi-Dirac statistics leading to the Pauli exclusion principle. Protons and neutrons are considered as moving freely within the nuclear volume. Collison of two identical particles will result in no net change in the overall energy configuration of the system. This is because any collison will only reflect the exchange of quantum states between two nucleons So, we can assume the nucleons are freely moving as collison has no impact. The binding potential is generated by all nucleons. In a first approximation, these nuclear potential wells are considered as rectangular: it is constant inside the nucleus and stops sharply at its end. Neutrons and protons are distinguishable fermions and are therefore situated in two separate potential wells. Each energy state can be occupied by two nucleons with different spin projections. All available energy states are filled by the pairs of nucleons (no free states , no transitions between the states). The energy of the highest occupied state is the Fermi energy E_F. The difference B' between the top of the well and the Fermi level is constant for most nuclei and is just the average binding energy per nucleon B'/A = 7–8 MeV.

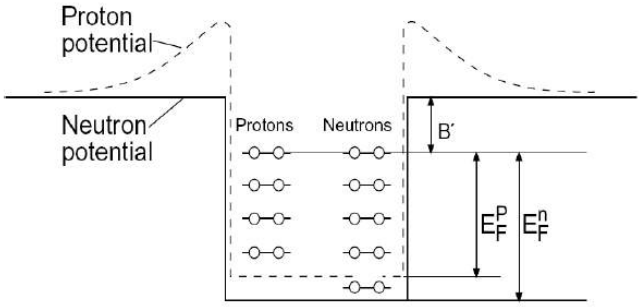

Figure 4: Figure showing rectangular potential wells and Binding energy and Fermi energy for protons and neutrons. The two potentials, though, have slightly different shapes, mainly because of the Coulomb part: The well for protons is less deep because of the Coulomb potential by the amount E_c and externally; the $1/r$ dependence of the Coulomb potential extends the range.

3.1 Fermi momentum and energy

Neglecting spin, the state's degeneracy n, i.e., the number of states of protons and neutrons within the spherical nuclear volume V is given by:

$$n = \frac{\iint d^3r d^3p}{(2\pi\hbar)^3} = \frac{V.4\pi \int_0^{p_{max}} p^2 dp}{(2\pi\hbar)^3} = \frac{V.4\pi p_F^3}{(2\pi\hbar)^3 3} = \frac{V \cdot p_F^3}{6\pi^2\hbar^3} \tag{1}$$

At temperature T = 0, i.e. for the nucleus in its ground state, the lowest states will be filled up to a maximum momentum, called the Fermi momentum p_F. The number of these states follows from integrating eqn from 0 to p_{max}=p_F. Since an energy state can contain two fermions of the same species, we can have

$$\textbf{Neutrons: } \boldsymbol{N = \frac{V \cdot p_F^3}{3\pi^2\hbar^3}} \text{ and } \textbf{Protons: } \boldsymbol{Z = \frac{V \cdot p_F^3}{3\pi^2\hbar^3}} \tag{2}$$

Let' s estimate Fermi momentum: $R = R_0 A^{\frac{1}{3}} \implies V = \frac{4\pi R^3}{3} = \frac{4\pi R_0^3 A}{3}$. So, The density of nucleons in a nucleus = number of nucleons in a volume V:

$$n = 2(\text{for 2 spin states}) \times \frac{V \cdot p_F^3}{6\pi^2\hbar^3} = 2 \cdot \frac{4\pi R_0^3 A}{3} \cdot \frac{p_F^3}{6\pi^2\hbar^3} = \frac{4A}{9\pi} \cdot \frac{R_o^3 p_F^3}{\hbar^3}$$

$$\boxed{\boldsymbol{p_F = \left(\frac{9\pi\hbar^3 n}{4AR_0^3}\right)^{\frac{1}{3}} = \left(\frac{9\pi n}{4A}\right)^{\frac{1}{3}} \cdot \frac{\hbar}{R_0}}} \tag{3}$$

After assuming that the proton and neutron potential wells have the same radius, we find for a nucleus with $n = Z = N = A/2$ the Fermi momentum p_F:

$$p_F = p_F^n = p_F^p = \left(\frac{9\pi}{8}\right)^{\frac{1}{3}} \cdot \frac{\hbar}{R_0} \approx 250 \text{ MeV/c}$$

The nucleons move freely inside the nucleus with large momentum! And corresponding Fermi energy: $E_F = \frac{p_F^2}{2M} \approx 33$ MeV where M denotes the nucleon mass ($M_n \approx M_p$).

3.2 Nuclear symmetry energy

Since the Fermi level of the protons and neutrons in a stable nucleus have to be equal (otherwise the nucleus would enter a more energetically favourable state through β-decay) and the depth of the potential well as it is experienced by the neutron gas is larger than of the proton gas due to columb interaction which implies there are more neutron states than proton states occupied explaining the fact that $N > Z$ for heavier stable nuclei.

The dependence of the binding energy on the surplus of neutrons may be calculated within the Fermi gas model. First we find the average kinetic energy per nucleon:

$$\langle E \rangle = \frac{\int_0^{E_F} E \cdot \frac{dn}{dE} dE}{\int_0^{E_F} \frac{dn}{dE} dE} = \frac{\int_0^{p_F} E \cdot \frac{dn}{dp} dp}{\int_0^{p_F} \frac{dn}{dp} dp} \text{ where } \frac{dn}{dp} = Const \cdot p^2 (\text{from })$$

$$\langle E_{kin} \rangle = \frac{\int_0^{p_F} E_{kin}(p) p^2 dp}{\int_0^{p_F} p^2 dp} = \frac{\int_0^{p_F} \frac{p^2}{2M} p^2 dp}{\int_0^{p_F} p^2 dp} = \frac{3}{5} \cdot \frac{p_F^2}{2M} \approx 20\text{MeV}$$

The total kinetic energy of the nucleus is therefore:

$$E_{\text{kin}}(N,Z) = N \langle E_{\text{n}} \rangle + Z \langle E_{\text{p}} \rangle = \frac{3}{10M} \left(N \cdot (p_{\text{F}}^{\text{n}})^2 + Z \cdot (p_{\text{F}}^{\text{p}})^2 \right)$$

$$E_{\text{kin}}(N,Z) = \frac{3}{10M} \frac{\hbar^2}{R_0^2} \left(\frac{9\pi}{4}\right)^{2/3} \frac{N^{5/3} + Z^{5/3}}{A^{2/3}} \text{ (from 2,3)}$$

where the radii of the proton and the neutron potential well have again been taken the same. Expanding this result around the symmetric case with $N = Z = A/2$. Taking $Z - N = \epsilon$ and, $Z + N = A$ we have:

$Z = \frac{A}{2}\left(1 + \frac{\epsilon}{A}\right)$ and $N = \frac{A}{2}\left(1 - \frac{\epsilon}{A}\right)$ with $\frac{\epsilon}{A} << 1$ and inserting expansion of $(1+x)^n = 1+nx+{}^nC_2x^2+...$ we get:

$$E_{\text{kin}}(N,Z) = \frac{3}{10M}\frac{\hbar^2}{R_0^2}\left(\frac{9\pi}{8}\right)^{2/3}\left(A + \frac{5}{9}\frac{(N-Z)^2}{A} + \cdots\right) \tag{4}$$

So, for a fixed A kinetic energy is minimum for $N = Z$. The first term corresponds to the volume energy; the second term has exactly the form of the assymmetry energy in the Beth-Weizsäcker mass formula. The asymmetry energy grows with the neutron (or proton) surplus, thereby reducing the binding energy.

4 From Spherical-Shell Model to Deformed-Shell Model

Deviations from the liquid drop model predictions are observed to occur in experimental data at particular 'magic' nucleon numbers (2,8,20,28,50,82, and 126). The largest separation energies, for the least bound nucleon, and the highest binding energies are found to occur for 'doubly magic' nuclei like ${}^{16}_{8}$O ${}^{48}_{20}$Ca and ${}^{208}_{82}$Pb etc. To explain these observations a nuclear 'shell model' was developed.

The Spherical-Shell Model belongs to the phenomenological single particle models (‚independent particle models'), i.e. a type of model of noninteracting particles in a mean-field potential. Experimental evidence for shell structure is the existence of magic nuclei: (2, 8, 20, 28, 50, 82, 126):

- a larger total binding energy of the nucleus,
- a large number of isotopes or isotones with the same magic number for protons (neutrons)
- a higher energy of the lowest excited states,
- a larger energy required to separate a single nucleon etc.

A phenomenological shell model is based on the Schrodinger equation for the single-particle levels i :

$$\left(-\frac{\hbar^2}{2M}\nabla^2 + V(r)\right)\psi_i(r) = \epsilon_i\psi_i(r)$$

$V(r)$ is a nuclear potential i.e. spherically symmetric, $\psi_i(r)$ - wave function and ϵ_i– energy eigenvalues. We try different types of potentials to explain the energy levels of the nucleus such as:

- the **Woods-Saxon potential:** $V(r) = -\frac{V_0}{1+e^{\left[\frac{r-R}{a}\right]}}$

  (with $V_0 = 50$Mev, R=1.1$A^{\frac{1}{3}}$fm and $a = 0.5$ fm)
- the **harmonic-oscillator potential:** $V(r) = \frac{1}{2}m\omega^2r^2$
- the **square-well potential:** $V(r) = \begin{cases} \mathbf{0} & \textbf{for } r \le R \\ +\infty & \textbf{for } r \le R \end{cases}$

We have already worked out that woods-saxon potential with spin-orbit term is able to produce the energy levels of the nucleus. Experimentalists found there is strong evidence of stable nuclear deformations. For example:

- Large quadrupole moments, that have been observed in nuclei far from the spherical closed shells.
- The existence of rotational bands, which require the presence of stable nuclear deformations.

To explain these we use a deformed average potential. The generalization of the phenomenological shell model to deformed nuclear shapes was first given by **S. G. Nilsson** in 1955, so this version is often referred to the **Nilsson model**. The idea is to make oscillator constants different in the different spatial directions i.e. $V(r) = \frac{m}{2}\omega_0^2R^2$. This is a ellipsoid with axes X,Y, and Z and given by: $\omega_o R = \omega_x X = \omega_y Y = \omega_z Z$. The condition for volume conservation is:

$$\frac{4}{3}\pi(\omega_o R)^3 = \frac{4}{3}\pi(\omega_o X)(\omega_o Y)(\omega_o Z) \implies R^3 = XYZ \implies \boxed{\boldsymbol{\omega_o^3 = \omega_x\omega_y\omega_z}}$$

Now assume axial symmetry around the z axis, i.e., $\omega_x = \omega_y$, and a small deviation from the spherical shape given by a small parameter δ. So, defining:

$$\omega_x^2 = \omega_y^2 = \omega_0^2(1 + \frac{2}{3}\delta), \quad \omega_z^2 = \omega_0^2(1 - \frac{4}{3}\delta)$$

such that volume conservation is satisfied i.e. $\left(\omega_0^2(1+\frac{2}{3}\delta)\right)^2 \omega_0^2(1-\frac{4}{3}\delta) \approx \omega_0^6$.
As we know the spherical harmonic

$$Y_{20}(\theta,\phi) = \sqrt{\frac{5}{16\pi}}(3\cos^2\theta - 1) = \sqrt{\frac{5}{16\pi}}(2z^2 - x^2 - y^2)\frac{1}{r^2}$$

Using this we can rewrite the potential as

$$\begin{aligned}
\boldsymbol{V(r)} =& \frac{m}{2}(\omega_x^2 x^2 + \omega_y^2 y^2 + \omega_z^2 z^2) \\
=& \frac{m}{2}(\omega_0^2(1+\frac{2}{3}\delta)x^2 + \omega_0^2(1+\frac{2}{3}\delta)y^2 + \omega_0^2(1-\frac{4}{3}\delta)z^2) \\
=& \frac{1}{2}m\omega_0^2 r^2 - \beta_0 m\omega_0^2 \boldsymbol{r^2 Y_{20}(\theta,\phi)} \text{ where, } \beta_0 = \frac{4}{3}\sqrt{\frac{4\pi}{5}}\delta
\end{aligned} \tag{5}$$

In the spherical shell model it was necessary to include a strong spin-orbit interaction and a term to 'flatten the bottom' of the potential, before agreement with experiment could be achieved. In order to include these effects in a deformed shell model potential, Nilsson added two terms to the anisotropic harmonic oscillator Hamiltonian such that in spherical coordinates the final Hamiltonian becomes:

$$\boxed{\hat{\boldsymbol{H}} = -\frac{\hbar^2}{2M}\boldsymbol{\nabla^2} + \frac{1}{2}\boldsymbol{m\omega_0^2 r^2} - \boldsymbol{\beta_0 m\omega_0^2 r^2 Y_{20}(\theta,\phi)} - \boldsymbol{\hbar\omega_0\kappa(2\hat{l}.\hat{s})} + \boldsymbol{\mu\hat{l}^2}} \tag{6}$$

The l^2 term is introduced phenomenologically to lower the energy of the single-particle states closer to the nuclear surface in order to correct for the steep rise in the harmonic-oscillator potential there. The Hamiltonian may be diagonalized in the basis of the harmonic oscillator using either spherical or cylindrical coordinates depending on the application:

- In **spherical coordinates** the spin-orbit and l^2 terms are diagonal, but the deformed oscillator potential doesn't.
- In **cylindrical coordinates** the deformed oscillator potential is diagonal and the angular-momentum terms must be diagonalized numerically.

Considering the quantum numbers resulting from both basis we have, the energy levels:

- In the **spherical basis**: $\boxed{\boldsymbol{\epsilon = \hbar\omega_0(N + \frac{3}{2})}}$ with the principal quantum number $N = 2(n_r - 1) + l$ where n_r is the radial quantum number, l is angular-momentum quantum number with projection m.
- In the **cylindrical basis:** $\boxed{\boldsymbol{\epsilon = \hbar\omega_z(n_z + \frac{1}{2}) + \hbar\omega_\rho(2n_\rho + |m| + 1)}}$ where n_z is the number of quanta in the z direction, n_r is that of radial excitations, and m is the angular momentum projection on the z axis.

The derivations for these energy level expression is given in **appendix**. Introducing the spin-orbit term $V_{ls} = C\hat{l}.\hat{s}$ we get:

$$\hat{l}.\hat{s} = \frac{1}{2}(\hat{l}+\hat{s})^2 - \hat{l}^2 - \hat{s}^2) = \frac{1}{2}\hbar^2[j(j+1) - l(l+1) - s(s+1)]$$

The splitting of the two levels with $j = l \pm \frac{1}{2}$,we have $E_{j=l+\frac{1}{2}} - E_{j=l-\frac{1}{2}} = C\hbar^2(l+\frac{1}{2})$. Experimentally we found that $E_{j=l+\frac{1}{2}} < E_{j=l-\frac{1}{2}}$ So, C has to be -ve depicting its attractive nature. C can be r dependent but mostly we take it to be a constant 0.3-0.6 MeV/$\hbar^2$.

The energy levels are labeled as nl_j: By the radial quantum number n, orbital angular momentum l, and total angular momentum j, The nl_j level is $(2j+1)$ times degenerate with projections $\Omega = -j, \ldots, +j$. There are two types of shell closures:

- **Closed j shell:** if all the projections Ω belonging to the same j state are filled.
- **Major shell closure:** if there is a larger gap in the level scheme to the next unfilled j shell, i.e., a magic number is reached.

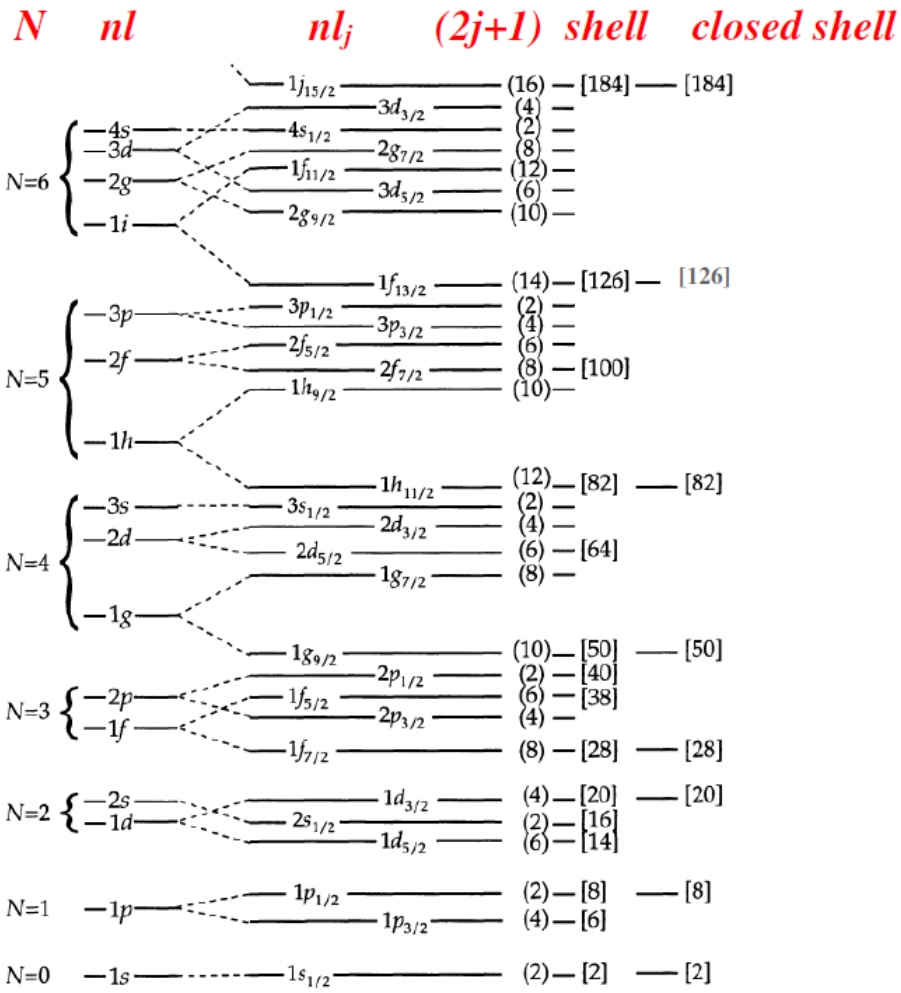

Figure 5: Level scheme for a harmonic oscillator with spin-orbit coupling:

For the spherical shape the levels are grouped according to the principal quantum number N (with the splitting by the spin-orbit force determined through the total angular momentum j), but the behavior with deformation depends on how much of the excitation is in the z direction. For prolate deformation, the potential becomes small in z direction, and the energy contributed by n_z excitations decreases. The cylindrical quantum numbers are thus helpful in understanding the splitting for small deformations. For very large deformations the influence of the spin-orbit and l^2 terms becomes less important and we can classify the levels according to the cylindrical quantum numbers. Label the single-particle levels with the set $\Omega^\pi[Nn_zm]$ where, the projection of total angular momentum Ω , and the parity π are good quantum numbers while N, n_z and m are only approximate and may be determined for a given level only by looking at its behavior near the spherical state.

The deformed shapes obtained in the **deformed shell-model** are different from those in the **collective model**, where the radius and not, as here, the potential, was expanded in spherical harmonics the shapes in the deformed shell model always remain ellipsoidal, even with arbitrarily long stretching, whereas in the collective model e.g. a fission shape is possible.

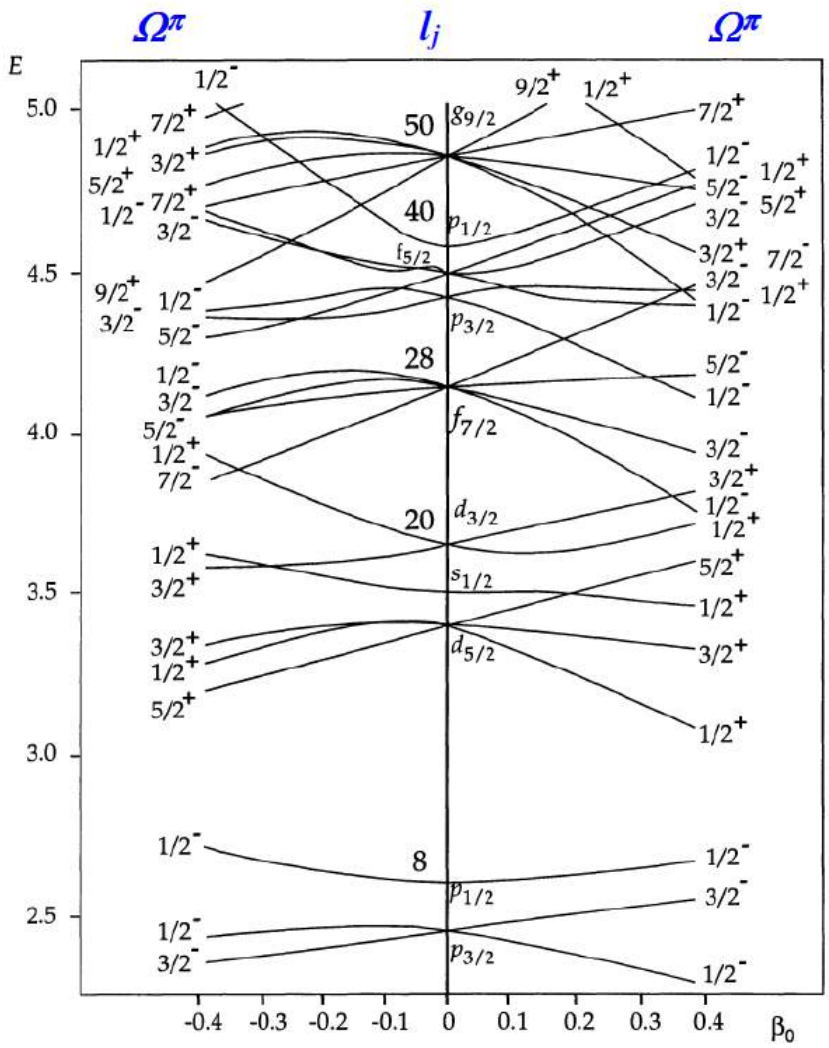

Figure 6: **Nilsson diagram** for the deformed shell model. The single-particle energies are plotted as functions of deformation β_0 and are given in units of $\hbar\omega_0$. The quantum numbers Ω^π for the individual levels and l_j, for the spherical ones are indicated as well as the magic numbers for the spherical shape.

5 Collective Nuclear Rotation

5.1 Rotational Bands and Band Crossings

Deformed nuclei exhibit collective rotational bands. The rotational motion involve contributions of many nucleons so, collective term is used. The excitation energy E, and the angular momentum,I are related as $E = \frac{\hbar^2}{2\mathscr{I}} I(I+1)$ where $\mathscr{I}$ is the moment of inertia. We can derive this formula by semi-classical treatment of a rigid rotor by solving the Schrödinger equation for rigid rotor in spherical coordinates. The series of states with consecutively increasing angular momentum is known as the 'rotational band'. The lowest state of the band is referred to as the **'bandhead'.** The state of lowest energy at a given angular momentum is called the **'yrast state'**. The locus of yrast states forms the '**yrast line**'. In an even-even nucleus at low rotational frequency the yrast band will be based on the ground state configuration, i. e. all the nucleons are in pairwise occupation of time-reversed orbits with the lowest excitation energy possible. The spin and parity of the ground state will be $I^\pi = 0^+$. The bandhead of the first excited band will correspond to a two-quasiparticle excitation. As the rotational frequency increases, the excitation energy of this first excited band may be lowered with respect to that of the ground state band until at some critical frequency, ω_{crit}, it becomes energetically favoured. This is known as the first band crossing. It can be explained by the effect of Coriolis force on two nucleons as shown in the figure.

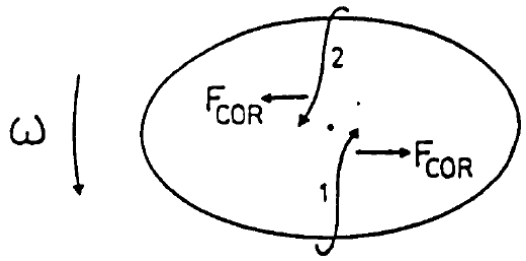

Figure 7: The effect of the Coriolis force, $F_{cor} = -2m(\overrightarrow{\omega} \times \overrightarrow{v})$ for two nucleons moving in time-reversed orbits. The force acts in opposite directions for each nucleon as the velocity of two nucleons are opposite to each other, tending to pull them apart and eventually breaking the pairing.

At the critical angular momentum, I_{crit},the pair will be broken and each nucleon may align its intrinsic angular momentum along the rotation axis. The nucleus can reduce its rotational frequency, ω, because of the gain of the intrinsic aligned angular momentum of the nucleons, i (this describes a backbend). The first excited band then becomes energetically favoured.

Near to the crossing point a plot of the excitation energy versus spin shows a characteristic behaviour. If the crossing takes place over one or two states the interaction between the bands is said to be weak and a plot of the moment of inertia, $\mathscr{I}$, versus ω^2 displays a backbend. If the crossing between the bands takes place over several more states the interaction between the bands is said to be strong, and the plot of the moment of inertia displays an upbend. The two situations are illustrated in following figure.

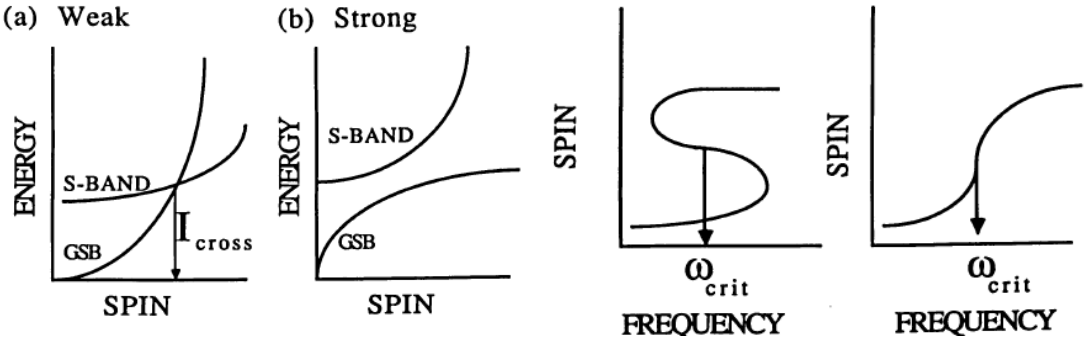

Figure 8: Schematic illustration of band interaction a) weak, b)strong.

5.2 Moments of Inertia

It is found empirically that the static moment of inertia for a rotating nucleus is typically 50-80% of the rigid body value. This is due in particular to the presence of pairing correlations. Two important quantities known as the nuclear moments of inertia can be introduced,[2], which reveal more about the intrinsic nuclear structure. The 'kinematic' moment of inertia is expressed by $\mathscr{I}^{(1)} = \hbar\frac{I_x}{\omega}$ and the 'dynamic' moment of inertia can be written as$\mathscr{I}^{(2)} = \left[\frac{1}{\hbar^2}\frac{d^2E}{dI^2}\right]^{-1} = \hbar\frac{dI_x}{d\omega}$. Here, I_x, represents the component of the total angular momentum on the rotation axis. The moments of inertia reflect the changes in a rotational band. The dynamic moment of inertia,$\mathscr{I}^{(2)}$, is very sensitive to alignment effects, whereas the kinematic moment of inertia, $\mathscr{I}^{(1)}$, describes the nuclear rotation at a given angular momentum, I, and rotational frequency, ω. For a rigid body the two quantities coincide.

5.3 Angular Momentum and Coupling Limits

The total angular momentum, I, of a rotating nucleus can be decomposed into two parts. The first is the angular momentum generated by the collective rotation of the inert even-even core, R. The second component is that generated by the intrinsic motion of the valence nucleons, J. Thus, it may be written that $\boldsymbol{I = R + J}$. In odd-mass nuclei, the intrinsic angular momentum of the valence nucleons, J, is non-zero (As odd-mass nuclei have an even no. of nucleons as core with a spin of zero but the second core is

formed by nucleons paired off having orbital and spin angular momentum of the last remaining nucleon). The excitation energies of the rotational system are given by

$$E_{rot} = \frac{\hbar^2}{2\mathscr{I}}(I-J)^2 = \frac{\hbar^2}{2\mathscr{I}}(I^2+J^2-2I.J) \tag{7}$$

The term $I.J$ represents the Coriolis interaction. Extreme limits of the nucleon-core coupling may then defined.

5.4 Cranking model

The deformed shell model (e.g. Nilsson Model) can be modified to include pairing. The cranking model is a model describing independent-particle motion in such a nucleus with both static deformed shape and pair fields and which is rotating. In such a rotating system fictive centrifugal and Coriolis forces emerge, resulting in important consequences for the shape and pair correlations. A very direct way of investigating the properties of a rotating nucleus is to force it to rotate with some fixed frequency, ω, or to "crank" the nucleus. The mathematical formulation of a rotating single-particle potential was first given by Inglis (1954). With the coordinates in the laboratory system given by x, y and z and those in the rotating system by x_1, x_2 and x_3, we get, for constant angular velocity, ω, around the x_1-axis,

$$\begin{aligned} x_1' &= x \\ x_2' &= x_2\cos\omega t + x_3\sin\omega t \\ x_3' &= -x_2\sin\omega t + x_3\cos\omega t \end{aligned}$$

The kinetic energy, T, of a particle with mass, m, at a position (x_1, x_2, x_3) is given by:

$$\begin{aligned} T &= \frac{m}{2}\left(\dot{x}_1^2+\dot{x}_2^2+\dot{x}_3^2\right) \\ &= \frac{m}{2}\left\{\dot{x}_1'^2+\dot{x}_2'^2+\dot{x}_3'^2-2\omega\left(\dot{x}_2'x_3'-\dot{x}_3'x_2'\right)+\omega^2\left(x_2'^2+x_3'^2\right)\right\} \end{aligned}$$

So, the lagrangian becomes $L = T - V\left(x_1', x_2', x_3'\right)$ and using the Lagrange equations $\frac{\mathrm{d}}{\mathrm{dt}}\frac{\partial \mathrm{L}}{\partial \dot{\mathrm{x}}_i'} - \frac{\partial \mathrm{L}}{\partial \mathrm{x'}_i} = 0$ we get:

$$\begin{aligned} \mathrm{m}\ddot{x}_1' &= -\frac{\partial \mathrm{V}}{\partial \mathrm{x}_1'} \\ m\ddot{x}_2' &= -\frac{\partial V}{\partial x_2'} + 2m\omega\dot{x}_3' + m\omega x_2^2 \\ m\ddot{x}_3' &= -\frac{\partial V}{\partial x_3}, -2m\omega\dot{x}_2' + m\omega^2 x_3' \end{aligned} \tag{8}$$

By introducing the rotational vector $\overline{\omega} = \omega\hat{x}_1'$,where $\hat{x}_1'$ is the unit vector along the x_1-axis these equations can be written in the condensed form:

$$m\ddot{\bar{r}}' = -\nabla V - 2m\bar{\bar{\omega}}\times\dot{\bar{\mathrm{r}}}' - m\bar{\omega}\times(\bar{\bar{\omega}}\times\bar{r}') \tag{9}$$

Coriolis Centrifugal

As we know the canonical momenta is $p_i' = \frac{\partial \mathrm{L}}{\partial \dot{\mathrm{x}}_i'}$. So the equations become:

$$\begin{aligned} p_1'^2 &= m^2\dot{x}_1'^2 \\ p_2'^2 &= m_2^2\dot{x}_2'^2 - 2m^2\omega\dot{x}_2'x_3' + m^2\omega^2 x_3'^2 \\ \mathrm{p}_3'^2 &= \mathrm{m}^2\dot{x}_3'^2 + 2\ \mathrm{m}^2\omega\dot{x}_3'\mathrm{x}_2' + \mathrm{m}^2\omega_2^2 x_2'^2 \end{aligned}$$

So, the hamiltonian in rotating frame becomes:

$$\begin{aligned}\mathrm{H}_{\omega}\left(x_i', p_i'\right) = \sum_i x_i' p' - L &= \sum_i \dot{x}_i' \frac{\partial L}{\partial \dot{x}_i'} - L \\ &= \sum_{\mathbf{i}} \frac{1}{2m} p_i'^2 + v\left(x_i'\right) - \omega\left(x_2' p_3' - x_3' p_2'\right) \\ &= H_0\left(x_i', p_i'\right) - \omega L_1' (\text{As } \bar{L}' = \bar{r}' \times \bar{p}')\end{aligned}$$

where H_0 is the hamiltonian of the system when $\omega = 0$ or the normal non-rotating Hamiltonian. We must also take into account of the spin $\bar{s}$ of the nucleus, which means we must replace L_1' with $J_1' = L_1' + S_1'$ giving the equation:

$$H_{\omega}\left(x_i', p_i'\right) = H_0\left(x_i', p_i'\right) - \omega J_1' \tag{10}$$

In a rotation-symmetric potential, the wavefunctions of the nonrotating single-particle potential have a well-defined projection quantum number, Ω, of the angular momentum on the symmetry axis, which we shall define as the z-axis. So, the cranking hamiltonian becomes $H_{\omega} = H_0 - \omega J_z$ and the eigenvalues become $e_i' = e_i - \omega\Omega_i$.

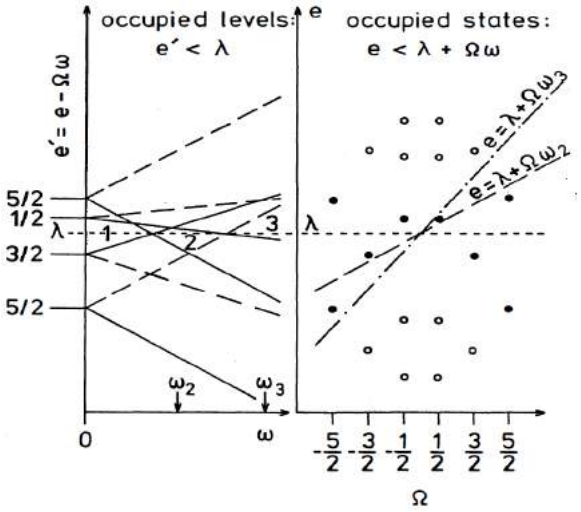

Figure 9: The left hand part of the figure shows in a schematic way a single-particle energy spectrum, resulting from a rotation around the nuclear synnnetry axis. $e_i' = e_i - \omega\Omega_i$.So, the graph is a straight line. All the energy levels, usually referred to as the single-particle **Routhians.** Slope Ω of the graph determines the projection of angular momentum on the rotation axis. and λ denotes the fermi level which is assumed to lie between the $\Omega = \frac{1}{2}$ and $\Omega = \frac{3}{2}$ at $\omega = 0$. And the two ω dependent energy levels emerging out of the left side figure corresponds to two directions of ω. (In the description of cranking presented above rotational states may be interpreted as quasiparticle excitations in a potential rotating uniformly with a rotational frequency, ω, about one of the principal axes (PA). The x-axis was used in the preceding description. However the idea of uniform rotation about a tilted axis (TA) has been shown to be very useful in describing the properties of high-K bands.[7, 6] where the cranking Hamiltonian is $H_{3D}^{\omega} = H - \overrightarrow{\omega}.\overrightarrow{I}$ with $\overrightarrow{\omega} = (\omega_1, \omega_2, \omega_3) = \omega(\sin\theta\cos\phi, \sin\theta\sin\phi, \cos\theta)$).

In the rotating system, the total energy is sum of the energies of all the levels below the Fermi energy, i.e. $E' = \sum_{i=1}^{N} e_i'$. N is the no. of nucleons. Energy in the lab frame is

$$E = \langle H_o \rangle = \langle H_{\omega} \rangle + \omega \langle J_z \rangle = E' + \omega J_z = \sum_{i=1}^{N} (e_i' + \omega\Omega_i) = \sum_{i=1}^{N} e_i$$

which is independent of the rotational frequency, ω. But e_i itself is ω dependent as we consider the energy of the levels only below the fermi level in the rotating frame i.e. $e_i' < \lambda$ or $e_i < \lambda + \omega\Omega_i$.

The eigenvalues of H_{ω}can be written as

$$e_{\mu}' = \langle \mu | H_{\omega} | \mu \rangle = \langle \mu | H_0 | \mu \rangle - \omega \langle \mu | J_x | \mu \rangle \tag{11}$$

which implies that

$$\frac{de'_\mu}{d\omega} = -\langle\mu|J_x|\mu\rangle = -I_x \tag{12}$$

Which implies that the slope of the single-particle Routhians is equal to the expectation value of the angular momentum operator J_x with reversed sign. For a system containing N nucleons the total angular momentum along the rotational axis is calculated as $I_x = \sum_{\mu=1}^{N}\langle\mu|J_x|\mu\rangle$ where μ is over all the occupied levels. For the yrast configurations this is normally the N lowest Routhians.

The total Routhian is given by:

$$E' = \sum_{\mu=1}^{N}\langle\mu|H_\omega|\mu\rangle = \sum_{i=1}^{N} e'_i \tag{13}$$

and similarly the total energy in the laboratory frame is obtained by taking the matrix element of H_0 for all the occupied eigenstates and adding them up i.e.

$$E = \sum_{\mu=1}^{N}\langle\mu|H_0|\mu\rangle = \sum_{\mu=1}^{N}\langle\mu|H_\omega|\mu\rangle + \omega\langle\mu|J_x|\mu\rangle = E' + \omega I_x \text{ (using 11)} \tag{14}$$

From 13 it is clear that The total routhian is continuous at the crossing frequency, but not its derivative which is clear from 12 and 13. Similarly, The total energy in the laboratory system is also discontinous because if we differentiate 14 with respect to I_x we get ω. So, the canonical relation becomes

$$\omega = \frac{dE(I)}{dI_x}$$

approximating the differential quotient by a quotient of finite differences (by restricting ourselves to sequences with ,$\triangle I = 2$, when defining a rotational band.) we get,

$$\omega(I) = \frac{E(I+1) - E(I-1)}{I_x(I+1) - I_x(I-1)}, \text{ where } I_x(I) = \sqrt{(I+\frac{1}{2})^2 - K^2}$$

to take into account the projection K of the angular momentum onto the symmetry axis. The value of K is set equal to the angular momentum of the band head.

6 Calculation of pair breaking frequencies in nuclei with both quadrupole and octupole deformations

The plots of $\mathscr{I}^{(2)}$ vs breaking frequency is attached below for all even-even and even-odd nuclei. Cranked shell-model calculations have been performed for a number of even-mass isotopes of Rn (Z=86) up to U (Z=92). The universal parameterization of the Woods-Saxon potential, incorporating quadrupole, octupole and higher-order degrees of deformation has been used. The purpose of these calculations is to obtain insights into the structure of these nuclei which are characterized by comparable magnitudes of quadrupole and octupole deformations. The values of the frequencies at which a pair of nucleons (either protons or neutrons) is broken due to the Coriolis force is obtained from the calculations. These values are compared with those from experiment, where data are available. In other cases, the calculations constitute predictions in regions which cannot presently be accessed by experiment.

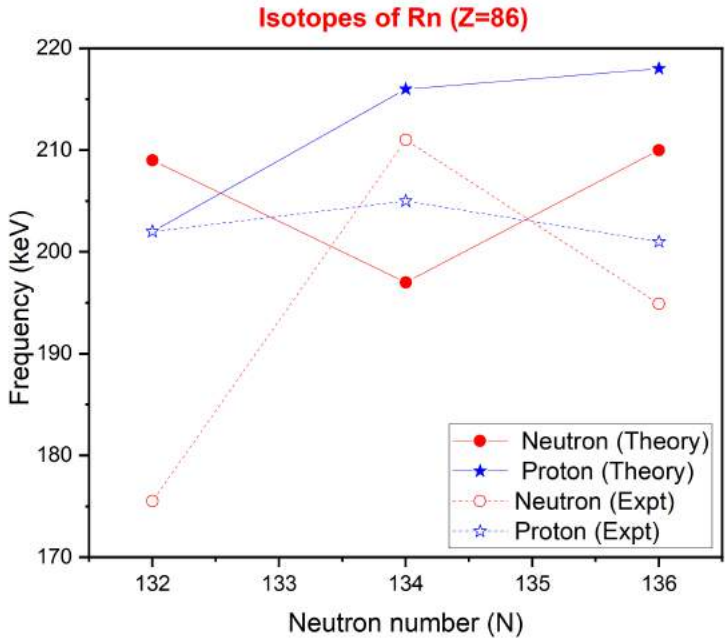

Figure 10: Rotational frequency for breaking a pair of nucleons in Rn isotopes from theoretical calculations performed in this work and their comparison with experimental values.

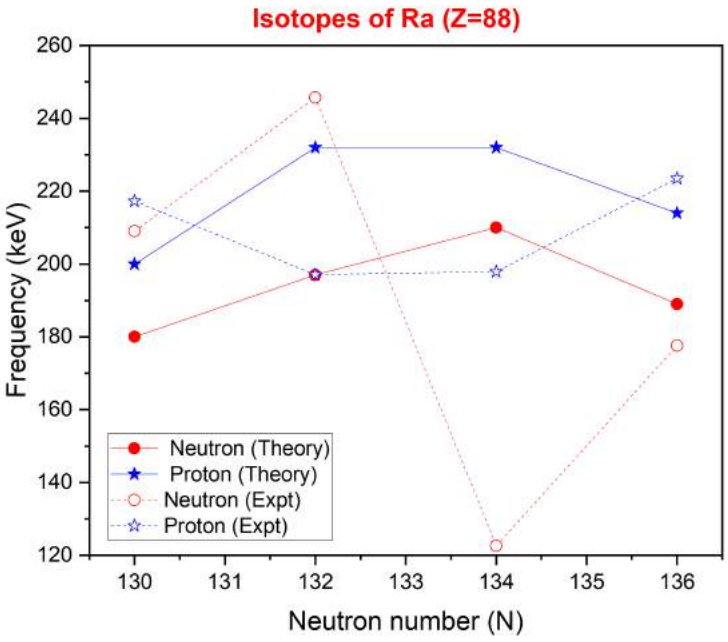

Figure 11: Rotational frequency for breaking a pair of nucleons in Ra isotopes from theoretical calculations performed in this work and their comparison with experimental values.

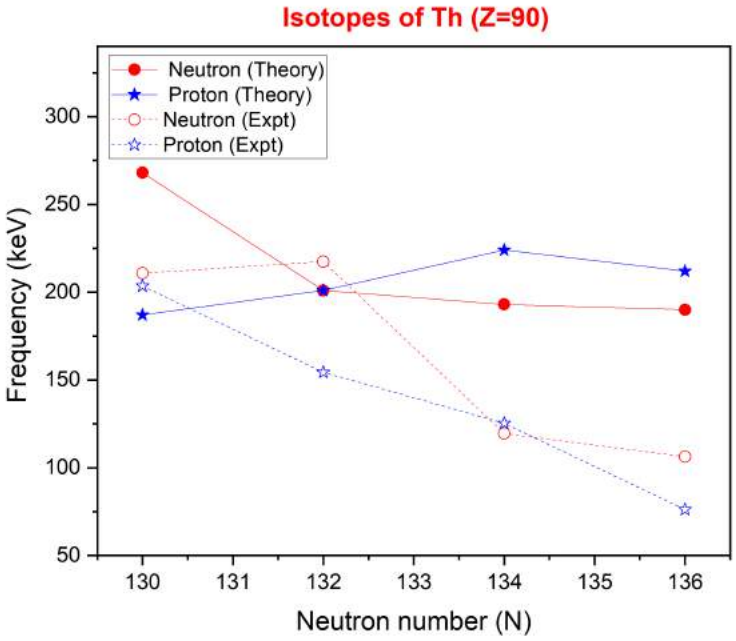

Figure 12: Rotational frequency for breaking a pair of nucleons in Th isotopes from theoretical calculations performed in this work and their comparison with experimental values.

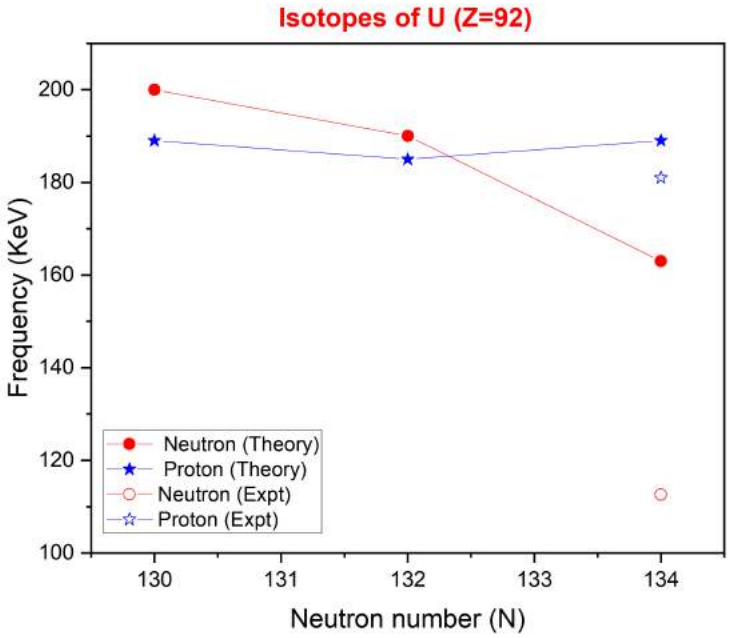

Figure 13: Rotational frequency for breaking a pair of nucleons in U isotopes from theoretical calculations performed in this work and their comparison with experimental values.

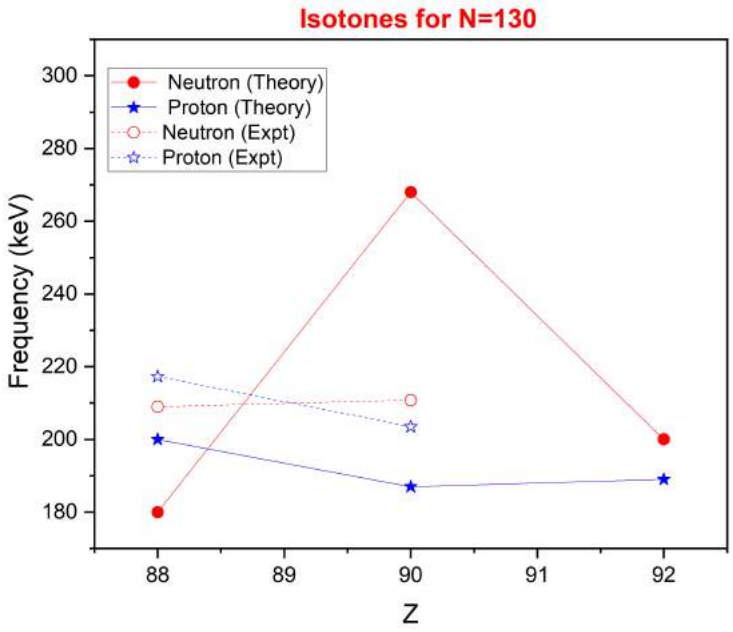

Figure 14: Rotational frequency for breaking a pair of nucleons in isotones for N=130 from theoretical calculations performed in this work and their comparison with experimental values.

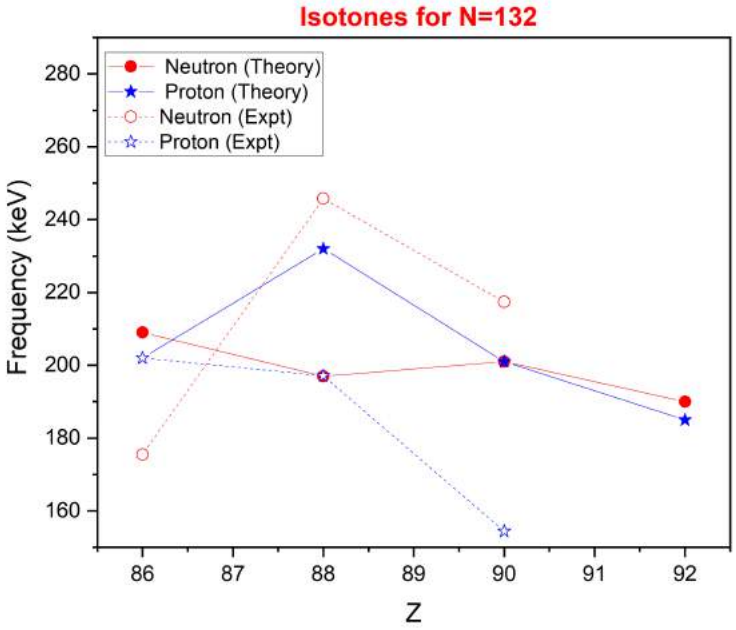

Figure 15: Rotational frequency for breaking a pair of nucleons in isotones for N=132 from theoretical calculations performed in this work and their comparison with experimental values.

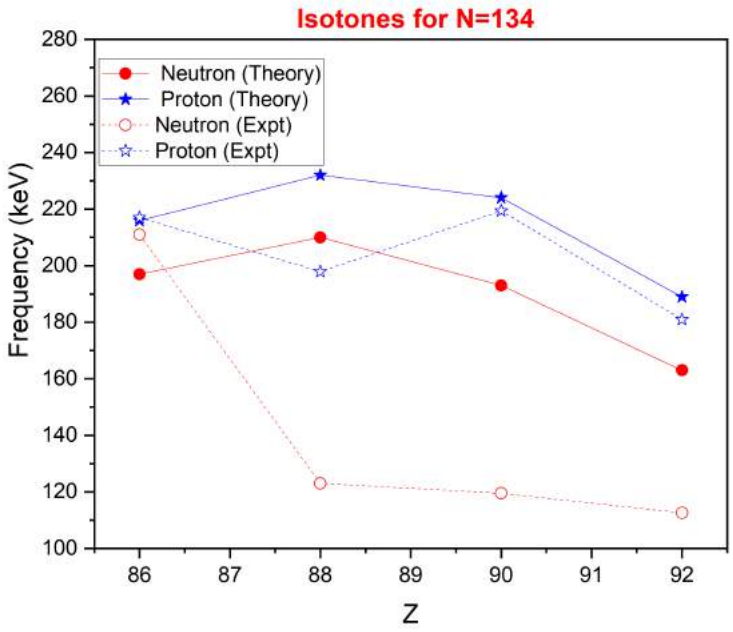

Figure 16: Rotational frequency for breaking a pair of nucleons in isotones for N=134 from theoretical calculations performed in this work and their comparison with experimental values.

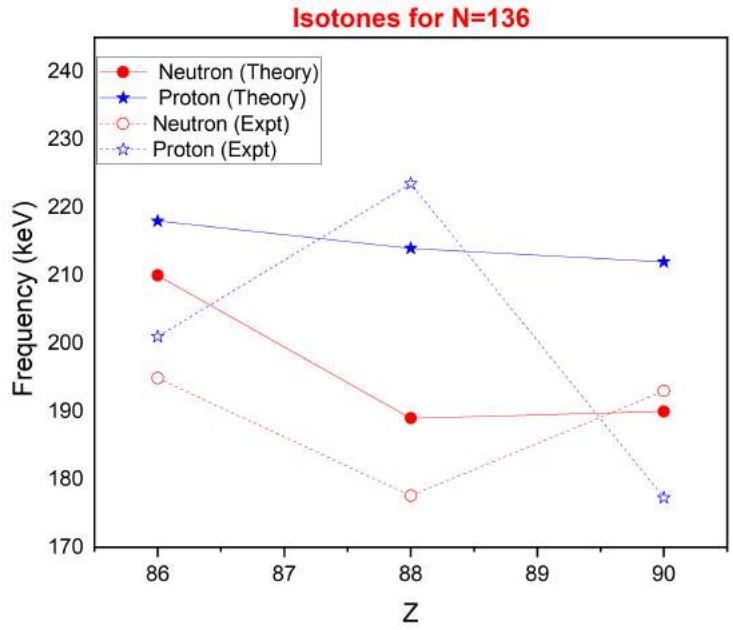

Figure 17: Rotational frequency for breaking a pair of nucleons in isotones for N=136 from theoretical calculations performed in this work and their comparison with experimental values.

The results for the odd-even cases are included below.

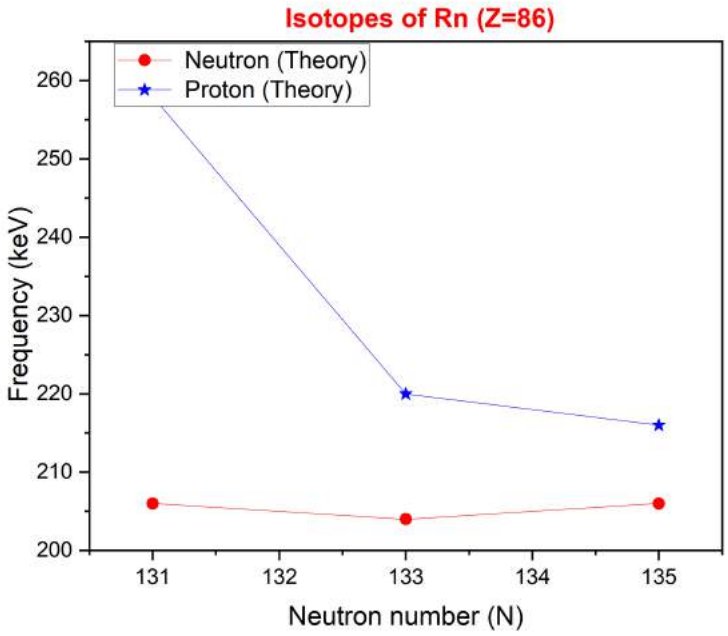

Figure 18: Rotational frequency for breaking a pair of nucleons in Rn isotopes from theoretical calculations performed in this work and their comparison with experimental values.

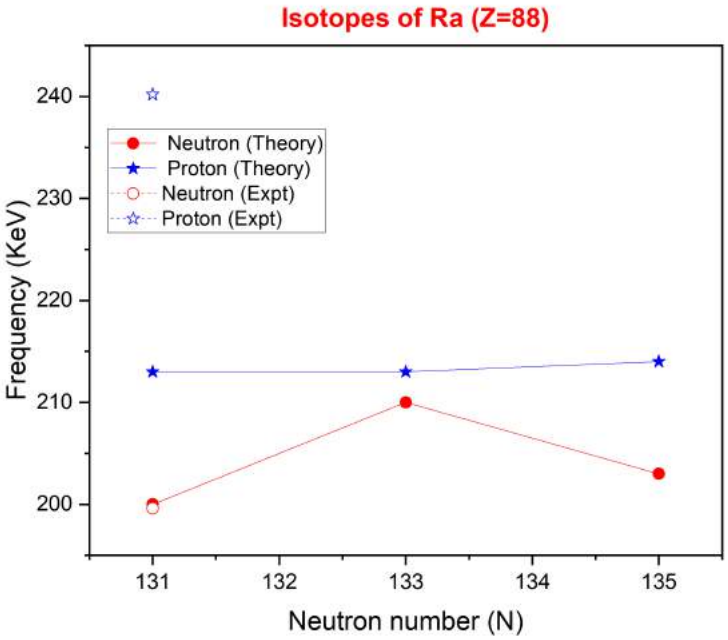

Figure 19: Rotational frequency for breaking a pair of nucleons in Ra isotopes from theoretical calculations performed in this work and their comparison with experimental values.

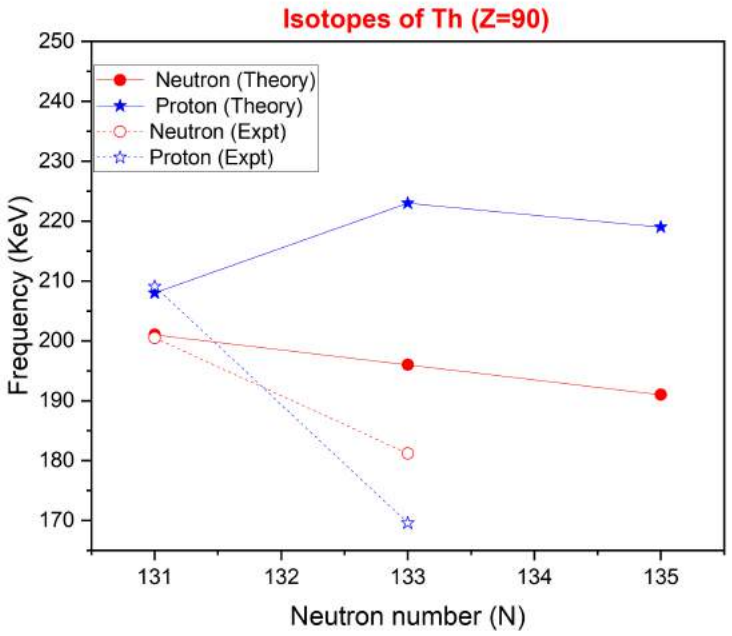

Figure 20: Rotational frequency for breaking a pair of nucleons in Th isotopes from theoretical calculations performed in this work and their comparison with experimental values.

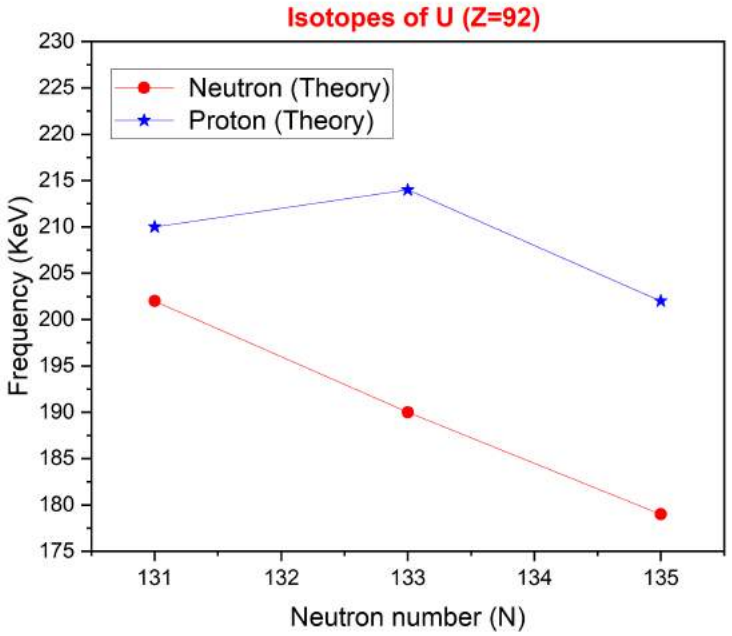

Figure 21: Rotational frequency for breaking a pair of nucleons in U isotopes from theoretical calculations performed in this work and their comparison with experimental values.

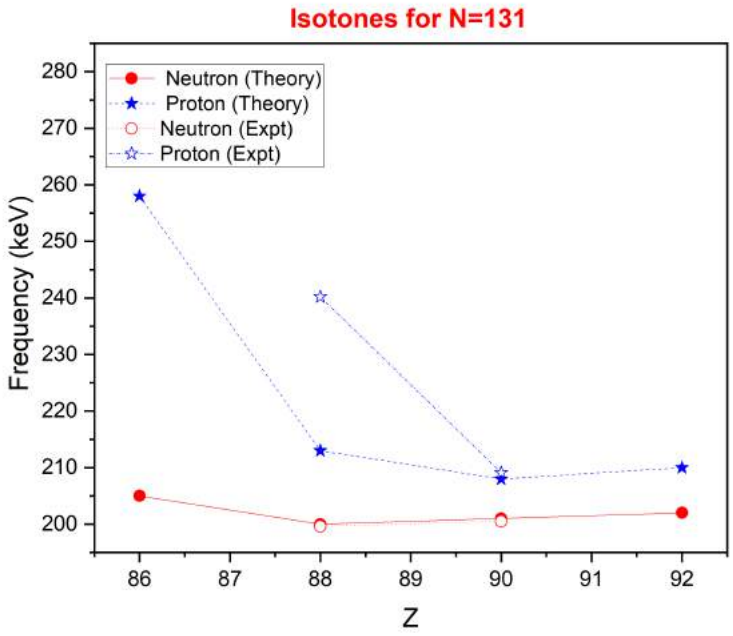

Figure 22: Rotational frequency for breaking a pair of nucleons in isotones for N=131 from theoretical calculations performed in this work and their comparison with experimental values.

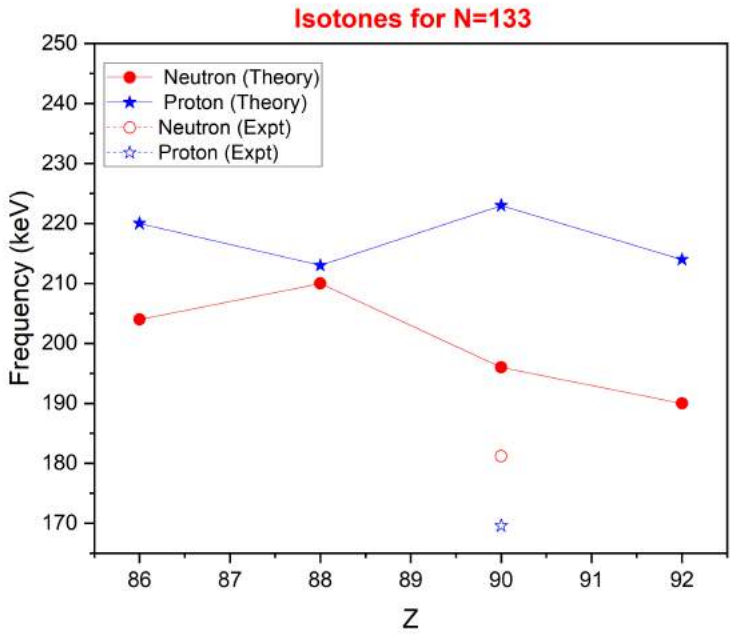

Figure 23: Rotational frequency for breaking a pair of nucleons in isotones for N=133 from theoretical calculations performed in this work and their comparison with experimental values.

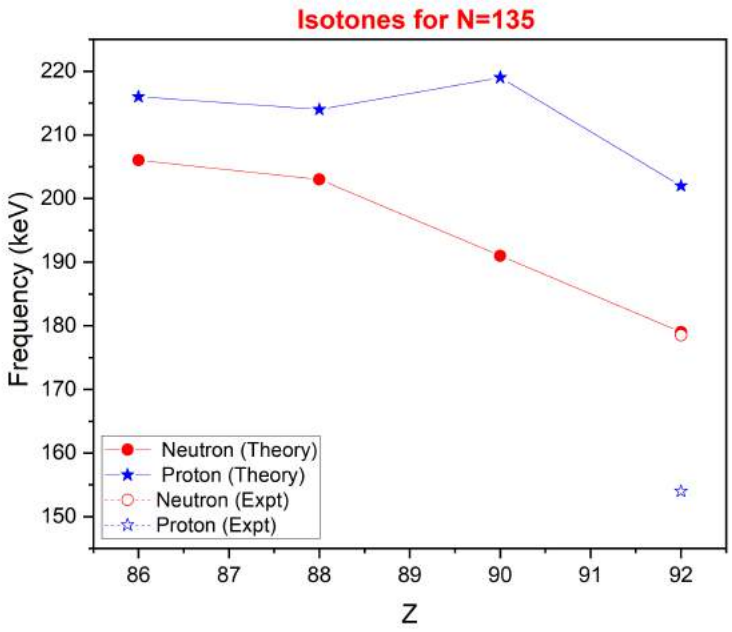

Figure 24: Rotational frequency for breaking a pair of nucleons in isotones for N=135 from theoretical calculations performed in this work and their comparison with experimental values.

References

[1] Shapes and Shells in Nuclear Structure S.G. Nilsson and I. Ragnarsson (Cambridge University Press) (1990)

[2] A. Bohr and B. Mottelson, Phys. Scr. 24 (1981)

[3] FUNDAMENTALS IN NUCLEAR PHYSICS by Khairi M-S. Abdullah, University of Duhok Publication

[4] Concepts of Nuclear Physics by B. L. Cohen

[5] INTRODUCTORY NUCLEAR PHYSICS by Kenneth S. Krane, Oregon State University

[6] S. Frauendorf and T. Bengtsson, International Symposium on Future Directions in Nuclear Physics, Strasbourg, AIP ConL Proc. (1991) pp223

[7] S. Frauendorf, in: Proc. 21st INS International Symposium on Rapidly Rotating Nuclei 1992, Tokyo; Nud. Phys. A, 557 (1993) 259c

[8] QUASIPARTICLE SPECTRA NEAR THE YRAST LINE by R. BENGTSSON and S. FRAUENDORF, Nuclear Physics A31:1 (1979) 139-171 ;

[9] THE CRANKING MODEL - Theoretical and Experimental Bases by R. Bengtsson and J.D. Garrett

A Appendix

A.1 In Cartesian Coordinates

To determine the eigenfunctions of the harmonic oscillator in Cartesian coordinates we write the Schrödinger equation as:

$$\left[-\frac{\hbar^2}{2m}\left(\frac{\partial^2}{\partial x^2}+\frac{\partial^2}{\partial y^2}+\frac{\partial^2}{\partial z^2}\right)+\frac{\omega^2}{2}\left(x^2+y^2+z^2\right)\right]\psi(x,y,z)=E\psi(x,y,z)$$

As the Hamiltonian in this case is simply the sum of three one-dimensional harmonic-oscillator Hamiltonians, the solution is a product of one-dimensional harmonic-oscillator wave functions:

$$\phi_n(\xi)=N_n\mathrm{e}^{-\frac{1}{2}\xi^2}\mathrm{H}_n(\xi)\quad,\quad N_n=\left(\sqrt{\pi}n!2^n\right)^{-1/2},\xi=x\sqrt{\frac{m\omega}{\hbar}}$$

$H_n(x)$ are the **Hermite polynomials:** $H_n(x)=(-1)^n e^{x^2/2}\frac{d^n}{dx^n}e^{-x^2/2}$ with oscillator quantum numbers n_x, n_y and n_z,

$$\psi_{n_xn_yn_z}(x,y,z)=\phi_{n_x}(x)\phi_{n_y}(y)\phi_{n_z}(z)$$

This corresponds to the given number of excitations in the respective coordinate direction and an energy of $\boxed{\boldsymbol{E_{n_xn_yn_z}=\hbar\omega\left(n_x+n_y+n_z+\frac{3}{2}\right)}}$.

All states with the principal quantum number $N=n_x+n_y+n_z$ are degenerate, i.e. the states with the same N (but different combinations of n_x, n_y and n_z) have the same energy E.

A.2 In Cylindrical Cordinates

To determine the eigenfunctions of the harmonic oscillator in Cylindrical coordinates we write the Schrödinger equation as:

$$\hat{\boldsymbol{H}}\boldsymbol{\psi}(z,\rho,\phi)=\boldsymbol{E}\psi(z,\rho,\phi)\left[-\frac{\hbar^2}{2m}\left(\frac{\partial^2}{\partial z^2}+\frac{\partial^2}{\partial\rho^2}+\frac{1}{\rho}\frac{\partial}{\partial\rho}+\frac{\partial^2}{\partial\phi^2}\right)+\frac{\omega^2}{2}\left(z^2+\rho^2\right)\right]\psi(z,\rho,\phi)=E\psi(z,\rho,\phi)$$

$$\Longrightarrow\ \left(\hat{\boldsymbol{H}}_z+\hat{\boldsymbol{H}}_\rho+\hat{\boldsymbol{H}}_\phi\right)\psi(z,\rho,\phi)=\left(\boldsymbol{E}_z+\boldsymbol{E}_\rho+\boldsymbol{E}_\phi\right)\psi(z,\rho,\phi)$$

The separation of variables $\psi(z,\rho,\phi)=\xi(z)\chi(\rho)\eta(\phi)$ leads to

$$\begin{cases}0=\left(\frac{\mathrm{d}^2}{\mathrm{d}\phi^2}+\mu^2\right)\eta(\phi)\\ 0=\left(\frac{\mathrm{d}^2}{\mathrm{d}\rho^2}+\frac{1}{\rho}\frac{\mathrm{d}}{\mathrm{d}\rho}-\frac{m^2\omega^2}{\hbar^2}\rho^2-\frac{\mu^2}{\rho^2}+\frac{2mA}{\hbar^2}\right)\chi(\rho)\\ 0=\left(\frac{\mathrm{d}^2}{\mathrm{d}z^2}+\frac{m\omega^2}{\hbar^2}z^2+\frac{2m(E-A)}{\hbar^2}\right)\zeta(z).\end{cases}\tag{15}$$

Here μ and A are separation constants (to be defined).

- **ϕ-dependent part:** the azimuthal quantum number $\mu=0,\pm1,\pm2,...$ (due to axial symmetry): $\eta_\mu(\phi)=\frac{1}{\sqrt{2\pi}}e^{i\mu\phi}$.
- **z-dependent part:** eigenenergy $E=\hbar\omega\left(n_z+\frac{1}{2}\right)+A$
- **ρ-dependent part:** look at the asymptotic behavior of the wave functions:

- For $\rho\to0$ the equation becomes

$$0=\left(\frac{\mathrm{d}^2}{\mathrm{d}\rho^2}+\frac{1}{\rho}\frac{\mathrm{d}}{\mathrm{d}\rho}-\frac{\mu^2}{\rho^2}\right)\chi(\rho)$$

Solved with $\chi(\rho)=\rho^\alpha\to\alpha=|\mu|$ (the negative sign has to be discarded since the wave function must go to zero at the origin).

For $\rho \to \infty$ the equation approches

$$0 = \left(\frac{\mathbf{d}^2}{\mathrm{d}\rho^2} + \frac{1}{\rho}\frac{\mathrm{d}}{\mathrm{d}\rho} - \frac{m^2\omega^2}{\hbar^2}\rho^2 \right) \chi(\rho)$$

a trial with $\chi(\rho) = \exp\left(-\beta\rho^2\right) \implies$

$$\left(4\beta^2 - \frac{m^2\omega^2}{\hbar^2}\right)\rho^2 - 4\beta = 0$$

In this limit we get $\beta = m\omega/2\hbar$.
Introduce $k = m\omega/h$

$$\text{trial function } \chi(\rho) = \mathrm{e}^{-\frac{1}{2}k\rho^2}\rho^{|\mu|}L(\rho)$$

should fulfill the orthogonality condition :

$$\int_0^\infty \mathrm{d}\rho\rho\mathrm{e}^{-k\rho^2}\rho^{2\mu}L^2(\rho) = 1$$

The appropriate orthogonal polynomials are Laguerre polynomials:

$$\int_0^\infty \mathrm{d}x\mathrm{e}^{-x}x^\alpha L_n^\alpha(x)^2 = 1$$

The final trial function:

$$\chi(\rho) = \mathrm{e}^{-\frac{1}{2}k\rho^2}\rho^{|\mu|}L_n^{|\mu|}\left(k\rho^2\right)$$

Inserting this equation to (15) we get:

$$x\frac{\mathrm{d}^2}{\mathrm{d}x^2}L_n^{|\mu|}(x) + (|\mu|+1-x)\frac{\mathrm{d}}{\mathrm{d}x}L_n^{|\mu|}(x) - \left(\frac{|\mu|+1}{2} + \frac{mA}{2k\hbar^2}\right)L_n^{|\mu|}(x) = 0 \text{ (where } \quad x \to k\rho^2)$$

Comparing the previous equation with the differential equation for the generalized Laguerre polynomials:

$$x\frac{\mathrm{d}^2}{\mathrm{d}x^2}L_n^\alpha(x) + (\alpha+1-x)\frac{\mathrm{d}}{\mathrm{d}x}L_n^\alpha(x) + nL_n^\alpha(x) = 0$$

with the condition for A:

$$A = \frac{\hbar^2 k}{m}(2n + |\mu| + 1) = \hbar\omega(2n + |\mu| + 1)$$

The new quantum number n (or denoted as n_ρ) can take values from $0, \ldots, \infty$. Finally: the eigenfunctions of the harmonic oscillator in cylindrical coordinates are given by

$$\psi_{n_z n_\rho \mu}(z,\rho,\phi) = N\exp\left[-\frac{1}{2}k^2\left(z^2+\rho^2\right)\right]\mathrm{H}_{n_z}(kz)\rho^{|\mu|}L_{n_\rho}^{|\mu|}\left(k\rho^2\right)\mathrm{e}^{\mathrm{i}\mu\phi}$$

where N is the normalization constant, $k = \frac{m\omega}{\hbar}$.
The energy of the levels is given by

$$E = \hbar\omega(n_z + 2n_\rho + |\mu| + \frac{3}{2})$$

The degeneracy of the levels is independent of the coordinate system used, and the same for the principal quantum number N which can be split up as

$$N = n_x + n_y + n_z = n_z + 2n_\rho + |\mu|$$
$$\text{where} \mu = 0, \pm 1, \pm 2, \ldots$$
$$n_\rho = 0, 1, 2, 3, \ldots$$
$$n_z = 0, 1, 2, 3, \ldots$$

Thus,

$$\boxed{\boldsymbol{E = \hbar\omega(N + \frac{3}{2})}}$$